Plasmonic Light-Harvesting Devices over the Whole Visible Spectrum

Alexandre Aubry,* Dang Yuan Lei, Antonio I. Fernández-Domínguez, Yannick Sonnefraud, Stefan A. Maier, and J. B. Pendry

The Blackett Laboratory, Department of Physics, Imperial College London, London SW7 2AZ

ABSTRACT On the basis of conformal transformation, a general strategy is proposed to design plasmonic nanostructures capable of an efficient harvesting of light over a broadband spectrum. The surface plasmon modes propagate toward the singularity of these structures where the group velocity vanishes and energy accumulates. A considerable field enhancement and confinement is thus expected. Radiation losses are also investigated when the structure dimension becomes comparable to the wavelength.

KEYWORDS Plasmonics, nanoparticles, broadband device, transformation optics

The effectiveness of light in many applications depends on converting its energy into some other form. The interface of optical fibers with electronics, solar cells, and photosynthesis are all instances of this conversion. In free space, a photon's energy spreads spatially over at least a cubic wavelength whereas electrical and chemical energy is much more concentrated by several orders of magnitude. Therefore, the conversion process requires some form of harvesting of light's energy if the process is to be efficient: collecting on a micrometer scale and concentrating to the nanoscale. Perhaps the most well-known instance is the Förster mechanism operating in the chlorophyll molecular system. In manmade devices, surface plasmons provide an ideal mechanism for this process.[1−4] They can show strong coupling to light but also can have wavelengths of only a few tens of nanometers. Here, we propose two plasmonic devices for the efficient harvesting of light and concentration of the energy to the nanoscale.

Ideally, our device should have a large cross section relative to its physical size and operate efficiently over a broad continuous spectrum of frequencies. The latter is a severe challenge for small devices that tend to be efficient collectors at just a few resonant frequencies.[3,5] For example, silver spheres have a very strong dipole resonance but an extremely narrow line width. A continuous spectrum is usually associated with infinite physical size. However, there are exceptions to this rule; some particles having a singular physical structure do show strong broadband interaction with light and we shall describe a systematic methodology for designing these particles.

Our strategy is as follows: start with an infinite plasmonic system that naturally shows a broadband spectrum and apply a mathematical transformation that converts the infinite structure into a finite one while preserving the spectrum. Transformation optics provides us with a very general set of transformations but here we shall concentrate on a specific subset: the conformal transformations. Our canonical system is a point dipole that can be located near a thin layer of plasmonic material (Figure 1a) or between two semi-infinite slabs of metal (Figure 1b). Although the surface plasmon spectrum of a plane surface is degenerate at ω_{sp}, the surface plasmon frequency, in a thin slab hybridization of surface plasmons on opposing surfaces creates a continuous spectrum.[4]
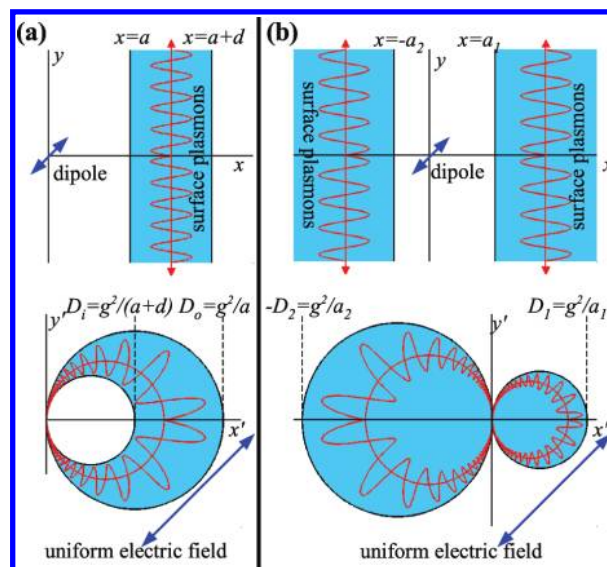

FIGURE 1. (Top) A thin layer of metal (a) and two semi-infinite metallic slabs separated by a thin dielectric film (b) support surface plasmons that couple to a dipole source, transporting its energy to infinity. The spectrum is continuous and broadband therefore the process is effective over a wide range of frequencies. (Bottom) The transformed materials of (a) and (b) are now a cylinder with cross section in the form of a crescent and two kissing cylinders, respectively. The dipole source is transformed into a uniform electric field.

* To whom correspondence should be addressed. E-mail: a.aubry@imperial.ac.uk. Phone: +44 (0)20 7594 7542. Fax: +44 (0)20 7594 2007.

The systems shown on top of Figure 1 have the desirable properties that we seek but have little practical utility. Now apply the following conformal transformation

$$z' = \frac{g^2}{z^*} \quad (1)$$

where $z = x + iy$ is the usual complex number notation and the superscript * stands for complex conjugate. Obviously all points at infinity in z translate to the origin in z' and planes translate into cylinders. Hence the resulting structures are a cylinder with a crescent shaped cross section (Figure 1a) and two kissing cylinders (Figure 1b). For the crescent, the diameters of the inner and outer cylinders are respectively

$$D_i = \frac{g^2}{d+a}, \ D_o = \frac{g^2}{a} \quad (2)$$

The diameters of kissing cylinders are respectively

$$D_1 = \frac{g^2}{a_1}, \ D_2 = \frac{g^2}{a_2} \quad (3)$$

For both structures, we define a key parameter r, which is the ratio between the inner and outer diameters of the crescent ($r = D_i/D_o$) and the ratio between the diameter of the smaller cylinder, D_1, and the overall physical size, $D = D_1 + D_2$, for the touching cylinders ($r = D_1/D$).

In the literature, flat crescent-shaped nanostructures have already been investigated,[6−12] but the case of a cylinder with a crescent-shaped cross-section has never been addressed to our knowledge. As we will see, this extended structure shows quite different properties compared to flat crescents, as, for instance, its ability of operating efficiently over a broadband spectrum of frequency. As to kissing cylinders, previous studies have investigated numerically the interaction between metallic nanowires.[13,14] Nevertheless, none of these works provide an analytical framework nor point out the broadband behavior that such devices may exhibit. As a general rule, the interactions between the two tips of a nanocrescent[7,10] or between two nanoparticles[13,15−20] have been investigated theoretically avoiding the "kissing" case, probably because of the occurrence of a singularity that makes numerical calculations more complex. On the contrary, conformal transformation provides an elegant tool to investigate such singular structures. Ross McPhedran and colleagues actually studied kissing cylinder pairs using conformal transformation and have shown the continuity of the spectrum contrary to the nontouching case.[21,22] However, they did not point out the spectacular light-harvesting and superfocusing properties that such singular plasmonic structures can exhibit as well as their potential applications.

Transformation of the dipole is equally interesting; see Figure 1. We have chosen the origin of our inversion at the center of the dipole. Thus the two charges comprising the dipole, very close to the origin in z, translate to near infinity in z', which gives rise to a uniform electric field at the crescent. If the original dipole had strength Δ then in the transformed frame, the electric field at the origin is given by

$$\mathbf{E_0}(z' = 0) = \frac{1}{2\pi\varepsilon_0}\frac{\Delta}{g^2} \quad (4)$$

We shall assume that the dimensions of the crescent and kissing cylinders are sufficiently small that the surface plasmon modes are well described in the near field approximation. In this case, the dielectric properties of these nanostructures are the same as those of the slab from which it is derived. Also preserved under the transformation is the electrostatic potential associated with an excitation

$$\phi(x, y) = \phi'(x', y') \quad (5)$$

However the field strength is not preserved but can be calculated from the conserved potential and the compression factor; the field strength varies as the compression and therefore the energy density scales as the square of the compression. This leads to a divergence of the energy density at the claws of the crescent and at the touching point of the two kissing cylinders, at least in a lossless system. The mathematics of the conformal transformation closely links the physics at work in each of the very different geometries. Solving the relatively tractable slab problem solves the crescent and kissing cylinders problem. First we pause to give a qualitative account.

On top of Figure 1, a dipole pumps energy into the surface plasmon modes of the metallic slab(s) that transport the energy out to infinity without reflection. The spectrum of modes is continuous with a lower bound at zero frequency and an upper bound at the bulk plasma frequency. At the surface plasmon frequency there is a singularity where the symmetry of the potential modes switches from antisymmetric to symmetric. The same modes are excited in the crescent and the kissing cylinders by a uniform electric field $\mathbf{E_0}$ (eq 4) that we shall take as due to an incident plane wave. Since we make the near-field approximation, all dimensions are less than the wavelength but the changed geometry means that the excited modes have a net dipole moment. This provides coupling to the external field. Transformation of the modes tells us that in the crescent, modes are excited mainly at the fat part of the crescent and propagate around
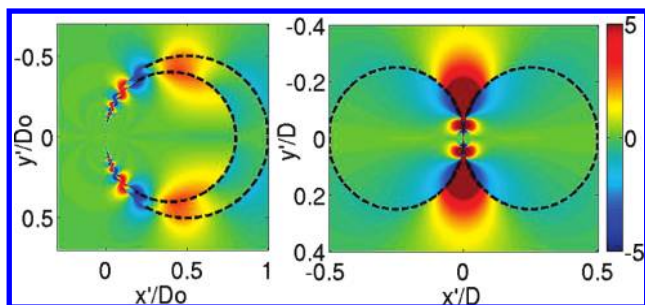
FIGURE 2. Amplitude of the x'-component of the electric field normalized by the incoming field (polarized along x'). The left and right panels display the field in the crescent (for $r = 0.8$) and in the two kissing cylinders (for $r = 0.5$), respectively, considering silver at $\omega = 0.9\omega_{sp}$. The color scale is linear and restricted to $[-5\ 5]$ but note that the field magnitude is by far larger around the singularity of the structures.
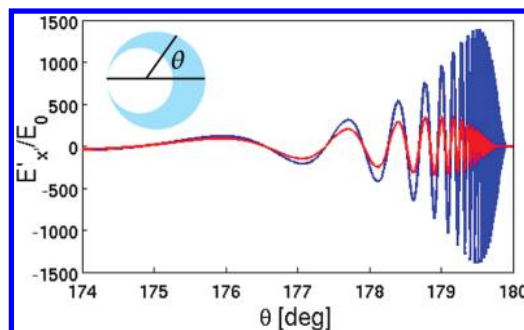

FIGURE 3. (Blue curve) Amplitude of the x'-component of the electric field at the surface of the crescent, plotted as a function of the angle, θ, defined in the figure, for $\omega = 0.75\omega_{sp}$ and $\varepsilon = -7.058 + 0.213i$ taken from Johnson and Christy.[23] Note that the field enhancement peaks at a finite angle. (Red curve) Losses are increased by a factor of 2 in the calculation $\varepsilon = -7.058 + 2 \times 0.213i$, resulting in less enhancement and a shift of the maximum to smaller angles. Both curves are normalized to the incoming field amplitude E_0. The crescent is defined by the ratio of diameters $r = 0.5$.
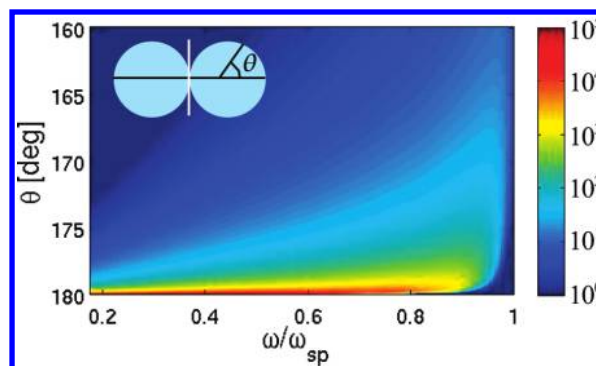

FIGURE 4. Absolute value of the field enhancement, $|E'|/E_0$, along the cylinder surface as a function of the angle θ and frequency for a plane wave incident normal to the axis of the cylinders. The two kissing cylinders are of same size ($r = 0.5$). The color bar is in log-scale.

to the claws in an adiabatic fashion (i.e., without being reflected). Similarly, the plasmon modes propagate along the surface of the kissing cylinders toward the touching point. Figure 2 illustrates this fact by showing our analytical calculation of the field distribution in the two nanostructures. For this figure as well as in the following of the study, the metal is assumed to be silver with a surface plasma frequency $\omega_{sp} = 3.67$ eV and permittivity taken from Johnson and Christy.[23] As surface plasmons propagate toward the structure singularity, their wavelength shortens and velocity decreases in proportion, similarly to what happens in sharp metallic tips or grooves.[24−26] Just as modes excited in the original slab never reach infinity in a finite time, modes excited in the crescent or in kissing cylinders never reach the tips or the touching point. In an ideal lossless metal, energy accumulates toward the singularity, its density increasing with time without bound. In practice, finite loss will resolve the situation leading to a balance between energy accumulation and dissipation. These devices are in many ways analogous to the "trapped rainbow" described by Ortwin Hess and colleagues.[27]

Figure 3 shows our analytic calculation of the electric field induced at the surface of the crescent by a plane wave polarized along the x' axis - see Figure 1. It is evident that losses truncate the growth of the field at a finite angle. In the case of silver for the given shape of crescent and frequency, the total field enhancement, $|E'|/E_0 = (E'^2_{x'} + E'^2_{y'})^{1/2}/E_0$, is a factor of 2×10^3 at an angle of $179.5°$. If this structure were deployed in a Raman scattering experiment,[28,29] sensitivity to molecules placed at the point would show an enhancement of 1.6×10^{13} in sensitivity. Also shown is a second calculation in which losses are increased by a factor of 2 greatly reducing the enhancement and decreasing the angle at which maximum enhancement occurs. Our analytic calculation predicts a maximum field enhancement scaling as the inverse square of the permittivity imaginary part ε_I. This is in agreement with the factor 4 observed between the blue and red curves in Figure 3.

Figure 4 displays the modulus of the field enhancement for two kissing cylinders as a function of frequency, calculated using the Johnson and Christy data.[23] At low frequencies, the field is strongly confined in the vicinity of the touching point and a spectacular field enhancement around 10^5 is predicted. This enhancement then decreases with frequency due to a larger damping when we approach the surface plasmon frequency. In the mean time, the electric field spreads spatially: the group velocity decreases with frequency and surface plasmons are absorbed before having reached the touching point.

Note that the field enhancements displayed by Figure 3 and Figure 4 may be unrealistic in practice. Indeed, at small length scales, continuum electrodynamics is no longer valid and nonlocal effects will play a role especially at the tips of the crescent, where the imaginary part of the dielectric function will increase.[30] In kissing cylinders, quantum mechanical effects, such as electron tunneling or screening, have also to be taken into account in the vicinity of the structure singularity and may reduce the field enhancement

relative to classical predictions.[31] Previous studies on nearly touching dimers actually predicted a divergence by a factor 5 of the field enhancement between the classical and quantum/nonlocal descriptions.[30,31]

In the near-field approximation, which holds when the dimensions of the crescent/kissing cylinders are less than the wavelength, the enhancement of electric field is independent of the size of the system. The magnitude of the enhancement is determined by how far around the nanostructure the wave field can propagate before being absorbed. Therefore as well as employing a low-loss metal it is also desirable to work at a frequency where the surface waves have a large group velocity so that they get as far as possible before being absorbed. By choosing the point on the crescent or on kissing cylinders at which the energy flow is intercepted, we can impedance match to almost any desired degree. Alternatively, if nonlinearity is the aim, the degree of nonlinearity observed can be tuned by the location of nonlinear material along the nanostructure. Such plasmonic device would also make an excellent detector of molecular species located near the claws; the broadband nature of the enhancement would lead to efficient concentration of the exciting radiation at the molecular site and efficient collector of emitted radiation, even if emitted at a very different frequency. The effect is already well-known in surface-enhanced Raman scattering experiments.

The energy pumped into the surface plasmons in the metal slab(s) (Figure 1) can be calculated from the scalar product of the induced electric field and the dipole[32,33]

$$P = -\frac{\omega}{2}\text{Im}\{\Delta^* \cdot \mathbf{E}(z=0)\} \tag{6}$$

This quantity can be calculated in the near field approximation by picking out the poles due to the propagating surface plasmon modes. This dipole power dissipated maps directly onto the power absorbed from a plane wave incident on the nanostructure in the transformed geometry. If eq 6 is normalized by the incoming flux $P_{in} = \varepsilon_0 c_0 |E_0|^2/2$, the absorption cross section $\sigma_a = P/P_{in}$ of the crescent can be deduced for $\varepsilon < -1$

$$\sigma_a = \frac{\pi^2\omega}{c_0}\left[\frac{rD_0}{1-r}\right]^2 \text{Re}\left\{\ln\left(\frac{\varepsilon-1}{\varepsilon+1}\right)\frac{4\varepsilon}{1-\varepsilon^2}\left(\frac{\varepsilon-1}{\varepsilon+1}\right)^{-2r/(1-r)}\right\} \tag{7}$$

Note that all orientations of the incident electric field are equally effective at excitation. This isotropy is allowed by the contact between the two crescent tips. On the contrary, an highly anisotropic behavior is expected as soon as the tips are no longer touching.[7-10] At the surface plasmon frequency where $\varepsilon = -1$, eq 7 is singular if $r < 1/3$, that is,
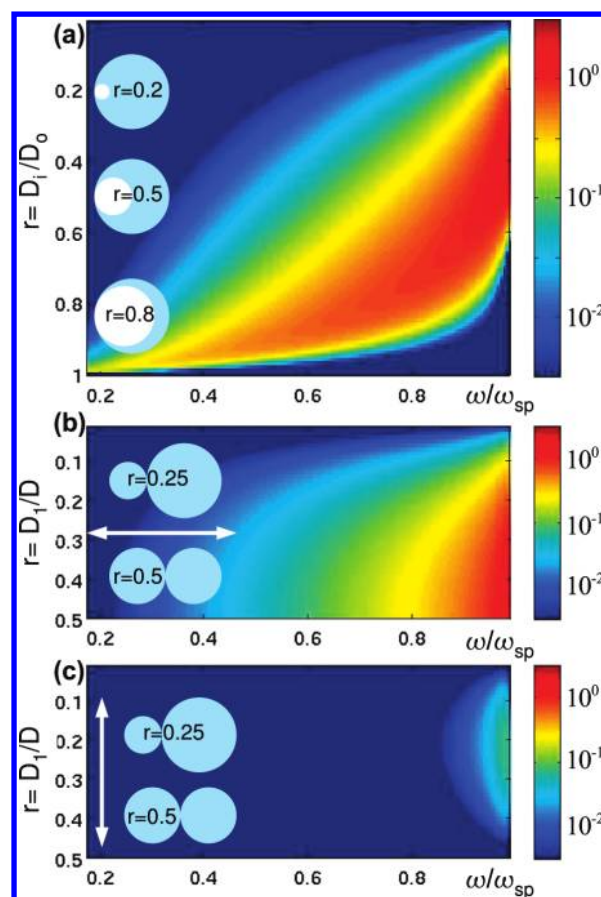

FIGURE 5. Absorption cross-section as a fraction of the physical cross-section as a function of r and frequency for the crescent (a) and the kissing cylinders with an incident electric field polarized along x' (b) and along y' (c). The overall size of each device is 20 nm. The color bars are in log-scale.

only for fat crescents. Figure 5a displays the absorption cross-section σ_a as a fraction of the physical cross section for $D_0 = 20$ nm. For $r > 1/3$, the crescent exhibits a broadband spectrum that shifts toward red when the crescent gets thinner. The efficiency of the crescent in light harvesting is also significant since its absorption cross-section is of the order of the physical cross-section even for such a small particle size ($D_0 = 20$ nm). For constant ratio r, σ_a/D_0 scales linearly with D_0. Thus higher cross sections could be obtained for larger diameter crescents, but in this case our near-field analytic theory may not be valid as we will see in the following.

The same analytical calculation can be performed for the two kissing cylinders. However, unlike the crescent this plasmonic device is strongly dependent on the polarization of the incoming field. Indeed, the two kissing cylinders geometry is derived from a metal−insulator−metal plasmonic structure (Figure 1). This configuration only supports odd surface plasmon modes for $\varepsilon < -1$.[4] If the dipole is placed at the center of the two metal slabs ($r = 0.5$), only its x-component can give rise to odd surface plasmon modes and its y-component is totally ineffective. In the transformed

geometry, it means that only the x'-component of the incident electric field can excite surface plasmons for two kissing cylinders of the same diameter ($r = 0.5$). Hence, the absorption cross-section strongly depends on the polarization of the incoming field, such that

$$\sigma_a^{x,y} = \frac{\pi^2 \omega}{c_0} r^2 (1 - r)^2 D^2 \mathrm{Re}\left\{ \ln\left(\frac{\varepsilon - 1}{\varepsilon + 1}\right) \left[\left(\frac{\varepsilon - 1}{\varepsilon + 1}\right)^{1-2r} + \left(\frac{\varepsilon - 1}{\varepsilon + 1}\right)^{2r-1} \pm 2 \right] \right\} \quad (8)$$

where σ_a^x and σ_a^y design the absorption cross sections for $\varepsilon < -1$ associated to the x' and y' components of the incoming field, respectively. σ_a^x and σ_a^y differ in the sign of the constant term in the square brakets of eq 8. Figure 5b,c display σ_a^x and σ_a^y as a fraction of the physical cross section for $D = 20$ nm. Similarly to the crescent, the two kissing cylinders are powerful light-harvesting devices over a broadband spectrum for an incident wave polarized along x', with a maximum efficiency for $r = 0.5$, that is, for two cylinders of the same size. On the contrary, the device exhibits a weak absorption cross-section if the incident wave is polarized along y'.

We now turn to the question of validity of the near-field approximation. To that aim, numerical simulations have been performed to investigate the effect of radiative losses when the structure dimension becomes comparable to the wavelength. All the numerical results presented have been obtained using COMSOL Multiphysics, a commercial software implementing the finite element method. Note that the mesh has to be carefully defined to accurately model the propagation of surface plasmon modes at the vicinity of the structure singularity. As in the analytical calculations, the optical response of silver was modeled through the fit of Johnson and Christy experimental data.[23]

Figure 6 compares the absorption spectra obtained numerically for different sizes of crescent and cylinder pair with the theoretical predictions. As σ_a and σ_a^x scale in D_0^2 (eq 7) and D^2 (eq 8), respectively, the absorption cross sections have been normalized by the square of the physical cross section to show explicitly the effect of radiation losses. For a dimension of 20 nm, the quasi-static approximation is verified and a good agreement is found between numerical and analytical results. Then, for larger dimensions (>100 nm), radiation damping becomes important and the absorption cross section falls compared to the analytical predictions derived under the electrostatic approximation. However, even though σ_a/D_0^2 and σ_a^x/D^2 decrease with the structure dimension, it should be emphasized that the absorption cross sections remain of the order of the physical cross section whatever the size of the device ($\sigma_a \sim D_o$, $\sigma_a^x \sim D$). Furthermore, the broadband behavior is kept and even improved for large structure dimensions. The continuity of the absorption spectrum is also highlighted by the compari-
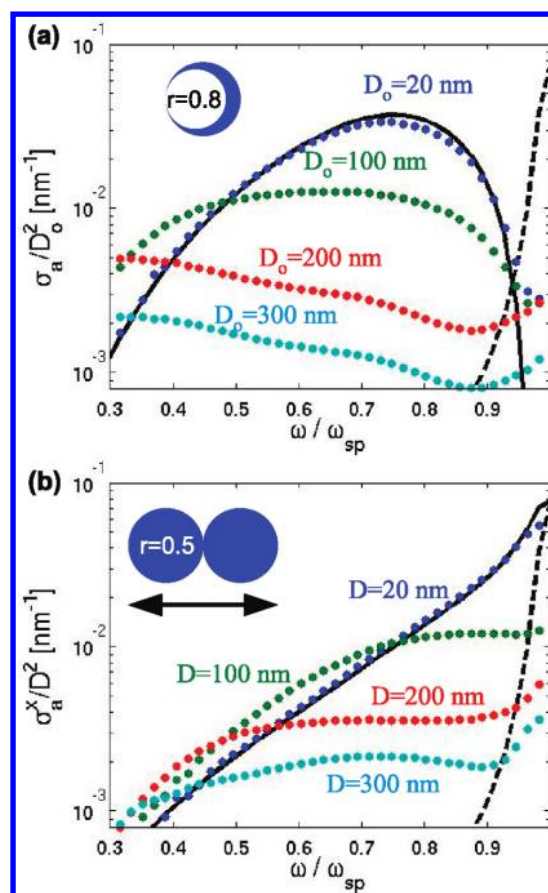

FIGURE 6. Absorption cross-section normalized by the square of the physical cross-section as a function of frequency for the crescent with $r = 0.8$ (a) and the kissing cylinders with $r = 0.5$ (b). The incident field is polarized along x'. The analytical absorption spectra (continuous black line) are compared to numerical results (dots) for different structure dimensions (20, 100, 200, 300 nm). The absorption spectrum of one individual cylinder[34] is also shown for comparison (dashed black line).

son with the single cylinder case in Figure 6. Note that radiation losses also affect the field enhancement in the nanoparticles. Whereas electrostatic theory predicts a field enhancement independent of the structure dimension, radiation losses break this property for $D > 100$ nm. A reduction of the field enhancement is then observed when the size of the system increases.

From an experimental point of view, the question of the sensitivity of such nanostructures to slight changes of the geometry can be raised. The degree of precision required should be in the order of the spatial confinement expected for the field. As to the absorption spectrum, its continuity relies on the contact between the tips of the crescent or between the cylinders. If there is no contact, a resonant feature will arise as suggested by previous numerical studies.[7,10,13,15−20]

To briefly conclude, this study shows how singular conformal transformation provides an elegant tool to design plasmonic structures capable of an efficient harvesting of light over the whole visible spectrum. Surface plasmon

modes are shown to propagate toward the structure singularity where the group velocity vanishes and energy accumulates. Strong field enhancement ($\sim 10^4$) and confinement are predicted within the classical approach. Numerical simulations have shown that such plasmonic structures are robust to radiation losses; the absorption cross-section is of the order of the physical cross-section over the whole visible spectrum for structure dimension up to 300 nm. The proposed plasmonic nanostructures would find great potential applications in solar cells, surface-enhanced Raman scattering, single molecular detection, and high-harmonic generation. The experimental challenge lies in the fabrication of such nanostructures with a nicely shaped singularity.

REFERENCES AND NOTES

(1) Barnes, W. L.; Dereux, A.; Ebbesen, T. W. *Nature* **2003**, *424*, 824–830.

(2) Bozhevolnyi, S. I.; Volkov, V. S.; Devaux, E.; Laluet, J.-Y.; Ebbesen, T. W. *Nature* **2006**, *440*, 508–511.

(3) Maier, S.; Atwater, H. A. *J. Appl. Phys.* **2005**, *98*, No. 011101.

(4) Maier, S. *Plasmonics: Fundamentals and Applications*; Springer: New York, 2007.

(5) Mie, G. *Ann. Phys.* **1908**, *25*, 377–445.

(6) Lu, Y.; Liu, G.; Kim, J.; Mejia, Y.; Lee, L. *Nano Lett.* **2005**, *5*, 119–124.

(7) Kim, J.; Liu, G.; Lu, Y.; Lee, L. *Opt. Express* **2005**, *13*, 8332–8338.

(8) Rochholz, H.; Bocchio, N.; Kreiter, M. *New J. Phys.* **2007**, *9*, 53.

(9) Bukasov, R.; Shumaker-Parry, J. *Nano Lett.* **2007**, *7*, 1113–1118.

(10) Ross, B.; Lee, L. *Nanotechnology* **2008**, *19*, 275201.

(11) Feng, L.; Orden, D. V.; Abashin, M.; Wang, Q.-J.; Chen, Y.-F.; Lomakin, V.; Fainman, Y. *Opt. Express* **2009**, *17*, 4824–4832.

(12) Wu, L. Y.; Ross, B.; Lee, L. *Nano Lett.* **2009**, *9*, 1956–1961.

(13) Kottmann, J.; Martin, O. *Opt. Express* **2001**, *8*, 655–663.

(14) García-Vidal, F.; Pendry, J. *Phys. Rev. Lett.* **1996**, *77*, 1163–1166.

(15) Hao, E.; Schatz, G. *J. Chem. Phys.* **2003**, *120*, 357–366.

(16) Nordlander, P.; Oubre, C.; Prodan, E.; Li, K.; Stockman, M. *Nano Lett.* **2004**, *4*, 899–903.

(17) Sweatlock, L.; Maier, S.; Atwater, H.; Penninkhof, J.; Polman, A. *Phys. Rev. B* **2005**, *71*, 235408.

(18) Romero, I.; Aizpurua, J.; Bryant, G.; de Abajo, F. G. *Opt. Express* **2006**, *14*, 9988–9999.

(19) Romero, I.; Teperik, T.; de Abajo, F. G. *Phys. Rev. B* **2008**, *77*, 125403.

(20) Lassiter, J. B.; Aizpurua, J.; Hernandez, L.; Brandl, D.; Romero, I.; Lal, S.; Hafner, J.; Nordlander, P.; Halas, N. *Nano Lett.* **2008**, *8*, 1212–1218.

(21) Phedran, R. M.; Perrins, W. *Appl. Phys.* **1981**, *24*, 311–318.

(22) Phedran, R. M.; Milton, G. *Proc. R. Soc. London, Ser. A* **1987**, *411*, 313–326.

(23) Johnson, P. B.; Christy, R. *Phys. Rev. B* **1972**, *6*, 4370–4379.

(24) Stockman, M. *Phys. Rev. Lett.* **2004**, *93*, 137404.

(25) Nerkararyan, K. *Phys. Lett. A* **1997**, *237*, 103–105.

(26) Pile, D. F. P.; Ogawa, T.; Gramotnev, D. K.; Okamoto, T.; Haraguchi, M.; Fukui, M.; Matsuo, S. *Appl. Phys. Lett.* **2005**, *87*, 061106.

(27) Tsakmakidis, K.; Boardman, A.; Hess, O. *Nature* **2007**, *450*, 397–401.

(28) Liu, G. L.; Lu, Y.; Kim, J. J. C.; Doll, L. P. L. *Adv. Mater.* **2005**, *17*, 2683–2688.

(29) Li, K.; Clime, L.; Cui, B.; Veres, T. *Nanotechnology* **2008**, *19*, 145305.

(30) de Abajo, F. J. G. *J. Phys. Chem. C* **2008**, *112*, 17983–17987.

(31) Zuloaga, J.; Prodan, E.; Nordlander, P. *Nano Lett.* **2009**, *9*, 887–891.

(32) Ford, G.; Weber, W. *Phys. Rep.* **1984**, *113*, 195–287.

(33) Jun, Y.; Kekatpure, R.; White, J.; Brongersma, M. *Phys. Rev. B* **2008**, *78*, 153111.

(34) Bohren, C.; Huffman, D. *Absorption and scattering of light by small particles*; John Wiley & Sons, Inc.: New York, 1983.